BMC Women's Health

RESEARCH

Open Access

Silencing circRNA-ZFAND6 induces trophoblast apoptosis by activating the mitochondrial pathway through the miR-575/SOD2 axis in unexplained recurrent spontaneous abortion

Wenting Wang[1†], Linxiang Huang[1†], Juan Lv[1], Zhijing Miao[1], Shuping Jin[1], Shan Li[1*] and Qing Cheng[1*]

Abstract

Background Unexplained recurrent spontaneous abortion (URSA) is a major problem in the field of human reproductive health. At present, several circRNAs have been reported to be differentially expressed and play an important biological function in pregnancy-related diseases. However, the role of circRNAs in URSA remains unclear.

Methods Levels of circRNA and miRNA were examined by RT-qPCR. The si-RNA and overexpression plasmid were respectively used to silence and overexpress circRNA-ZFAND6. We investigated the biological function of circRNA-ZFAND6 on trophoblasts through CCK8, EdU, Flow cytometric assay, Wound-healing assays and Transwell. Dual luciferase activity assay was conducted to identify the interaction between miR-575 and circRNA-ZFAND6.

Results We confirmed that circRNA-ZFAND6 was a stable circular RNA and was mostly localized in the cytoplasm. CircRNA-ZFAND6 was downregulated in placental villous tissues of URSA. CCK-8 and EdU assays showed that circRNA-ZFAND6 promoted the proliferation of HTR-8/SVneo cells. Flow cytometry and western blot assays prompted that circRNA-ZFAND6 obviously reduced cells apoptosis. Scratch wound healing and transwell assays revealed that circRNA-ZFAND6 had no effect on cell migration and invasion. CircRNA-ZFAND6 worked by adsorbing miR-575 through the ceRNA mechanism. MiR-575 can inhibit the proliferation and promote the apoptosis of HTR8/SVneo cells. SOD2 was identified as a direct target of miR-575 and was associated with mitochondrial apoptosis. Transmission electron microscopy, TMRM and ROS staining assays both suggested that circRNA-ZFAND6 affected mitochondrial apoptosis. Excessive trophoblast apoptosis was a key event to promote the development of URSA.

†Wenting Wang and Linxiang Huang contributed equally to this work.

*Correspondence:
Shan Li
lishan@njmu.edu.cn
Qing Cheng
qqingrr@163.com

Full list of author information is available at the end of the article

Conclusion CircRNA-ZFAND6, which is low expressed in URSA and regulates the apoptosis of trophoblast cells, may affect the expression of SOD2 and thus affect mitochondrial apoptosis by regulating miR-575. This is closely related to the occurrence of URSA.

Keywords CircRNA-ZFAND6, Hsa_miR_575, SOD2, URSA, Pregnancy loss

Background

Recurrent spontaneous abortion (RSA) is generally defined as two or more times of fetal loss before 24 weeks of gestation with the same spouse [1, 2]. It affects 1-5% of couples, bringing serious impact to patients and their families [3]. The etiology of RSA is complex, including genetic factors, uterine anatomic defects, autoimmune diseases, endocrine disorders, genital infections, thrombophilias, clinical factors and environmental factors [4]. However, these known factors account for only 50-60% of women with RSA, that is, despite considerable effort has been carried out to explore its causes and the potential pathogenesis, 40–50% cases of RSA remain unexplained [5, 6]. These cases are known as unexplained recurrent spontaneous abortion (URSA).

URSA has always been a hot and difficult issue in the field of obstetrics and gynecology. In recent years, clinical practice and existing research findings have found that the constituent ratio of causes of two and three spontaneous abortions is similar, therefore, it emphasizes the continuity of and the risk of recurrence of spontaneous abortion [7–9]. Previous research found that the risk of pregnancy loss in future increased with the number of previous miscarriages, and the incidence of miscarriage in the next pregnancy of patients with RSA is as high as 40-80% [10, 11], which causes great physical and mental trauma to patients and brings heavy burden to family and society. Currently, there are no effective clinical prevention and treatment means. Hence, it is of great value to explore the mechanism of URSA in order to find effective intervention.

Non-coding RNAs (ncRNAs) have become the center of attention as a novel biomarker for disease prediction, diagnosis and treatment [12]. Therefore, they are implicated in the etiology of a variety of pregnancy-related disorders, such as URSA [13]. Along with the fast development of high-throughput sequencing and bioinformatics, a class of closed covalent circular RNA (circRNA) has become the latest research hotspot due to the advantages of good stability and strong specificity. As a class of small noncoding RNAs, microRNAs (miRNAs) can bind to complementary sequences on target mRNAs, promoting mRNA degradation or translational repression [14]. Several functions of circRNAs have been identified. They can sponge miRNAs or compete endogenous RNAs, regulate gene transcription, translate proteins and bind to RNA-binding proteins [15–17]. CircRNAs promote RSA occurrence and development by affecting trophoblast proliferation, apoptosis, invasion, metastasis and placental angiogenesis [18]. For example, Zhu et al. revealed that circPUM1 may affect the occurrence and development of RSA by promoting trophoblast cellular processes and reducing inflammation through miR-30a-5p/JUNB axis [19], Gao et al. demonstrated that circFOXP1 could promote proliferation, inhibit apoptosis, and facilitate EMT- related migration and invasion of trophoblastic cells via regulating the miR-143-3p/S100A11 axis [20], furthermore, Liu et al. disclosed that circFBXW4 sponged miR-324–3p, regulating TJP1 expression, cell proliferation and invasion [21]. The role of differentially expressed circRNAs in URSA remains unknow.

The proliferation, apoptosis, invasion and migration of trophoblast cells are the key steps of blastocyst implantation and placentation [22, 23]. Increasing studies have shown that excessive trophoblast apoptosis can lead to or aggravate trophoblast dysfunction, promoting the development of URSA [24, 25]. In this study, we selected circRNA-0000643 for further study because it was significantly downregulated in placental villous tissues of URSA. We found that circRNA-0000643/miR-575/SOD2 axis functioned in the occurrence of URSA. It is expected to provide a new theoretical basis for the occurrence of URSA, and provide potential intervention targets for clinical diagnosis and treatment of URSA.

Materials and methods

Human sample

Placenta villous tissue samples were collected from 30 pairs of age-matched URSA patients and normal pregnant patients (with no history of spontaneous abortion, preeclampsia, ectopic pregnancy, preterm delivery, and systemic diseases) and 4 women who experienced missed abortion (unrecognized intrauterine death of the embryo or fetus without expulsion of the products of conception) for the first time in Women's Hospital of Nanjing Medical University (Nanjing Maternity and Child Health Care Hospital) between January 2022 and December 2023. The gestational age of all the pregnant women was between 6 and 12 weeks. Detailed information of patients was shown in Fig. 1i. Every participant provided informed consent. The Ethics Committee of Nanjing Maternity and Child Health Care Hospital permitted this study (No. [2021] NFKSL-076). All tissues were stored in liquid nitrogen after removing from patients for the following experiments.

Total RNA isolation and quantitative real-time PCR (RT-qPCR) analysis

Total RNA samples from cells and tissues were extracted by Trizol (Invitrogen, Carlsbad, CA, USA) according to the manufacturer's instructions. Then, those RNA was reverse transcribed into complementary DNA (cDNA) with a HiScript Reverse Transcriptase kit (Vazyme, Nanjing, China). Then, RT-qPCR reactions were performed by SYBR Green master mix (Invitrogen) in an ViiA7 real-time PCR system (Life technologies corporation, Gaithersburg, MD, USA). Obtained data were calculated by $2^{-\Delta\Delta Ct}$ method to represent the relative expression levels of the RNAs. MiRNA expressions were normalized to U6, and circRNA and mRNA expressions were normalized to GAPDH. The primer sequences for RT-qPCR which were commissioned to Sangon Biotech Co., LTD (Shanghai, China) were presented in Table S1 (miRNA and U6 were reverse transcribed adopting the stem-loop method, and the primers were purchased from Guangzhou RiboBio Biotechnology Co., LTD which did not provide primer sequences due to patent protection).

Cell culture and transfection

A human extravillous trophoblast cell line, HTR-8/SVneo and a human embryonic kidney cell line, HEK-293T (American Type Culture Collection, Manassas, VA, USA) were cultured in DMEM (Gibco, Carlsbad, CA, USA) containing 10% fetal bovine serum (FBS) (Gibco) and maintained at 37 °C in a humidified atmosphere with 5%CO2. Transient transfection was performed with a 50-60% cell density. Small interfering RNA (si-RNA), circRNA-0000643 over-expression plasmids, miR-575 mimics, miR-575 inhibitor and their related control were constructed by RiboBio (Guangzhou, China). Detailed sequence information was shown in the Table S1. We use Lipofectamine 3000 Transfection Kit (Invitrogen) to transfect siRNAs and overexpression plasmid. Transfected for 48 h, the protein and total RNA of the cells were harvested and subsequent functional experiments were carried out.

RNase R digestion assay and actinomycin D assay

A total of 5 μg total RNA extracted from HTR8/SVneo cells was incubated at 37 °C for 30 min with or without RNase R (Beyotime, Shanghai, China) and then inactivated at 70 °C for 10 min. Total RNA was collected for RT-qPCR analysis. HTR8/SVneo cells were exposed to 2 μg/mL actinomycin D (MedChem Express, Monmouth Junction, NJ, USA) at specified time points. Total RNA of different groups of cells was collected for RT-qPCR analysis.

Western blot analysis

A bicinchoninic acid (BCA) protein assay kit (Beyotime) was utilized to check the total protein concentrations after extracting by radioimmunoprecipitation assay (RIPA) lysis buffer. Then, total protein was boiled with a 5×loading buffer (Beyotime) at 95 °C for 5 min. The protein samples of equivalent amount were separated by 10% SDS-PAGE and transferred to polyvinylidene fluoride (PVDF) membranes (Millipore, Billerica, MA, USA). The membranes were blocked in 5% skimmed milk in TBST for 1 h and then they were incubated at 4 °C overnight with appropriate dilutions of specific primary antibodies against GAPDH (Biosharp, BL006B), Bax (Abcam, ab32503), Bcl-2 (Abcam, ab32124), SOD2 (Abcam, ab137037), Caspase9 (CST, #9504) or Cleaved-caspase3(CST, #9661). Subsequently, the membranes were further incubated with the HRP-conjugated secondary antibody (Beyotime; 1:2,000) at room temperature for 2 h and finally visualized with an enhanced chemiluminescence (ECL) detection system (Millipore). The level of protein expression was analyzed by Image J.

Cell proliferation assay

Cell proliferation ability was assessed by cell counting kit-8 (CCK-8) assays and EdU assays. About 5,000/well transfected HTR8/SVneo cells were put into 96-well plates to and cultivated at 37 °C for 0, 24, 48, or 72 h. At indicated time points, 10 μl CCK-8 reagent (Dojindo, Kumamoto, Japan) was seeded to each well and the cells were cultured for another 2 h. The optical density (OD) values were measured with a microplate reader (BioTek, Biotek Winooski, Vermont, USA) at 450 nm. The EdU assay was conducted by the BeyoClick™ EdU-555 Cell proliferation detection kit according to the protocol (Beyotime). Briefly, the EdU solution (10μM) was added to the 6-well plate and waited for 2 h at 37 °C. The cells were treated with 500 μl click reaction solution after being fixed with 4% paraformaldehyde. Cell nuclei was stained by Hoechst 33,342. Typical images were obtained by a fluorescence microscope (Zeiss, Germany).

Scratch wound healing assay

Scratch wound healing assay was conducted in order to measure the cell migration capability. Firstly, transfected cells were seeded in 6-well culture plates and cultivated till cells reached 80–90% confluence. Then, a vertical wound in each well was made by a 200 μl pipette tip. Pictures of the wound were taken at 0, 36 and 48 h. The wound area was measured using the ImageJ software.

Transwell migration and matrigel invasion assays

We performed the migration assay with a Transwell chamber (Corning, NY, USA) and the invasion assay with a Transwell chamber precoated with 60 μl Matrigel (BD

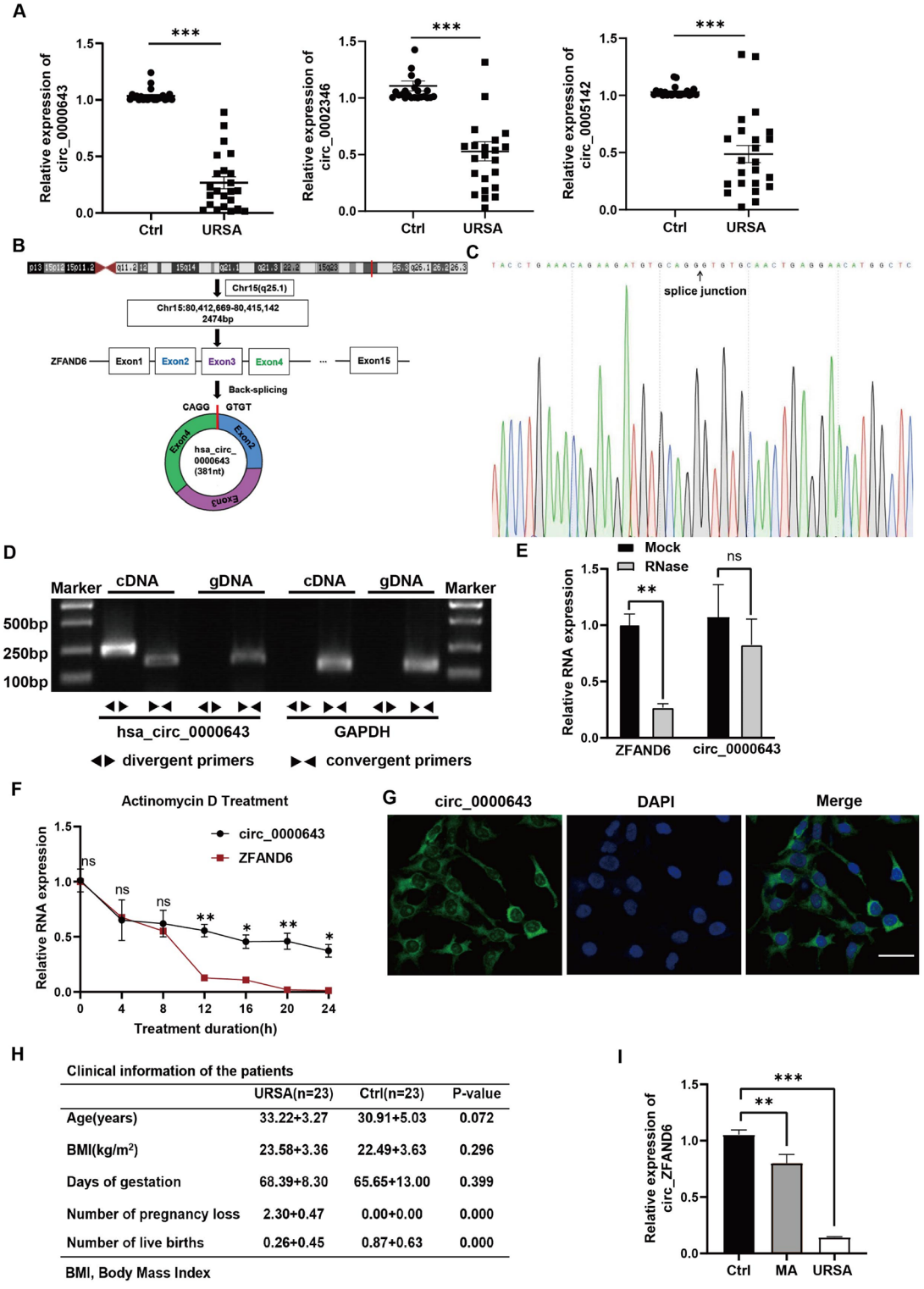

	URSA(n=23)	Ctrl(n=23)	P-value
Age(years)	33.22+3.27	30.91+5.03	0.072
BMI(kg/m²)	23.58+3.36	22.49+3.63	0.296
Days of gestation	68.39+8.30	65.65+13.00	0.399
Number of pregnancy loss	2.30+0.47	0.00+0.00	0.000
Number of live births	0.26+0.45	0.87+0.63	0.000

BMI, Body Mass Index

Fig. 1 (See legend on next page.)

Biosciences, San Jose, CA, USA) diluted with serum-free medium in a 24-well plate. Then, 150 µl of serum-free cell suspension containing $5 \times 10^{\wedge}4$ transfected cells were added to the upper chamber and 600 µl DMEM containing 10%FBS were added to the bottom chamber. After culturing the cells at 37 °C for 24 h, we collected cells for migration and after for 48 h, we collected cells for invasion. Then, the upper chamber was fixed with

(See figure on previous page.)

Fig. 1 CircRNA-ZFAND6 is downregulated in placental villous tissues of URSA patients. (**A**) RT-qPCR analysis of the expression of hsa_circ_0000643, hsa_circ_0005142, hsa_circ_0002346, in 23 paired villi tissues from normal pregnant (Ctrl) and URSA groups. (**B**) Schematic diagram exhibited the formation of hsa_circ_0000643. (**C**) Sanger sequencing of the RT-PCR products of hsa_circ_0000643. The black arrow indicated the splicing site of hsa_circ_0000643. (**D**) RT-qPCR products using divergent and convergent primers showed the circularization of hsa_circ_0000643. GAPDH was used as a negative control. (**E**) The levels of circular and linear ZFAND6 were detected by using RT-qPCR in HTR8/SVneo cells treated with RNase R. (**F**) RT-qPCRanalysis of the hsa_circ_0000643 and ZFAND6 expression in HTR8/SVneo cells under the treatment with actinomycin D. (**G**) RNA FISH detected hsa_circ_0000643's subcellular localization in HTR8/SVneo cells. Nuclei was stained with DAPI. Scale bar, 20 μm. (**H**) Clinical characteristics of the patients. (**I**) Expression of hsa_circ_ZFAND6 in 4 groups of villus tissues of NP group (Ctrl), first missed abortion group (MA) and URSA group. Three different independent experiments with three technical repetitions were performed. Data were expressed as the mean ± SEM. * $p<0.05$, ** $p<0.01$, *** $p<0.001$, ns, not significant

methanol for 10 min on ice and then stained with 0.1% crystal violet for 15 min. Representative images were obtained in three randomly selected fields under an inverted light microscope (Zeiss), and the number of cells penetrating the Matrigel and membrane was calculated.

Flow cytometry

Measurement of the apoptosis ratio of cells was carried out by flow cytometry with an Annexin V-FITC/PI Apoptosis Detection Kit (Vazyme). Briefly, transfected HTR8/SVneo cells (2 × 10^5 cells/well) were digested by trypsin without EDTA and then washed twice with ice-cold PBS. After resuspended in 100 μl 1×binding buffer, cells were stained in darkness with 5 μl Annexin V-FITC and 5 μl PI for 10 min at 20–25 °C. Eventually, flow cytometry was used to analyze the rate of cell apoptosis.

Fluorescence in situ hybridization (FISH)

The Cy3-labeled has_circ_0000643 probes were designed and synthesized by RiboBio to detect its subcellular location. Probes were hybridized to cells with the help of a Fluorescent in Situ Hybridization Kit (RiboBio). Images were obtained on a confocal laser scanning microscope (Leica, Wetzlar, Germany);

Dual luciferase reporter (DLR) assay

The wild type (WT) and mutation (Mut) 3'UTR of hsa_circ_0000643/SOD2 were inserted into the firefly-tagged pmiR-RB-Report™ luciferase vector (RiboBio), named as hsa_circ_0000643/SOD2-WT/Mut. MiR-575 mimics/mimics-NC were co-transfected with the reporter plasmid into HEK-293T cells by Lipofectamine 3000 (Invitrogen). The luciferase activity was sequentially measured after 48 h by the Dual Luciferase Reporter Assay Kit (Vazyme). Firefly luciferase activity was normalized to renilla luciferase activity.

ROS and TMRM measurement

ROS levels were measured by the ROS Assay Kit (Dojindo) according to the instructions. Cells were rinsed with HBSS and then were incubated with highly sensitive DCFH-DA Dye working solution (Dilution 1000 times) at 37 °C for 30 min. After washing with HBSS two times to remove extracellular DCFH-DA, typical photos were taken by a confocal laser scanning microscope (Leica). To detect mitochondrial membrane potential, treated cells were incubated with TMRM working solution (Dilution 1000 times) (Invitrogen) at 37 °C for 30 min and then cells were washed twice with PBS. Images were obtained by a fluorescence microscope (Zeiss). Alternatively, we digested the cells for flow analysis.

Statistical analysis

SPSS software (version 26.0) and GraphPad Prism (version 7.0) were applied in this study. All data was shown as mean ± SEM which was obtained from results of at least three independent experiments. Student's t-test or one-way ANOVA was utilized for two-group or multiple-group comparisons to acquire statistical differences. Statistical differences with P-value < 0.05 were considered statistically significant.

Results

CircRNA-ZFAND6 is downregulated in placental villous tissues of URSA patients

Our previous study screened differentially expressed circRNAs in URSA and normal pregnancy women by gene chip technology [26]. The results showed that a total of 594 circRNAs were differentially expressed by 2 times or more in placental villous tissues of patients with URSA compared with the normal pregnancy (NP) group. According to the results, we chose three differentially expressed circRNAs, hsa_circ_0000643, hsa_circ_0002346 and hsa_circ_0005142. To verify their expression in tissues, we collected 23 pairs of villi tissues from URSA and normal pregnancy (Ctrl) women for qPCR analysis and found that hsa_circ_0000643 was the most significantly decreased (Fig. 1A). Therefore, we selected hsa_circ_0000643 for further analysis.

Hsa_circ_0000643 consists of 381 nucleotides and is originated from exon 2, 3 and 4 of human ZFAND6 in chr15 (80412669–80415142) (Fig. 1B). To confirm the head-to-tail splicing of hsa_circ_0000643, we conducted Sanger sequencing (Fig. 1C). Trans-editing is a common cause of head-to-tail splicing, but genomic rearrangements can also form head-to-tail splicing, thus, we further designed convergent primers and divergent primers for hsa_circ_0000643 to amplify it using complementary DNA (cDNA) and genomic DNA (gDNA) from HTR8/SVneo cells as the template. Results showed

that only the divergent primers from cDNA can amplify hsa_circ_0000643 (Fig. 1D). Then, we designed primers for ZFAND6 and hsa_circ_0000643 in order to detect the stability of hsa_circ_0000643. We use RNase R to treat the RNA extracted from HTR8/SVneo cells and results showed that hsa_circ_0000643 was more resistant to RNase R exonuclease digestion (Fig. 1E). Furthermore, after treating HTR8/SVneo cells with actinomycin D (an inhibitor of transcription) for different times, hsa_circ_0000643 showed greater stability and resistance than ZFAND6 mRNA (Fig. 1F). All these evidences suggested that hsa_circ_0000643 was a circular RNA. FISH analysis revealed that the majority of hsa_circ_0000643 localized in the cytoplasm (Fig. 1G). Therefore, we renamed this RNA circRNA-ZFAND6. The clinical characteristics of 23 pairs of patients were shown in Fig. 1H. No differences were found between Ctrl and URSA group in terms of age, body mass index and days of gestation. However, URSA group showed a higher number of pregnancy loss and a lower number of live births than Ctrl group ($p < 0.01$). In addition, we found that the reduction of circRNA-ZFAND6 was more pronounced in the URSA group compared with the first missed abortion (MA) group (Fig. 1I). It was possible that the decrease in circRNA-ZFAND6 was more significant as the number of miscarriages increases.

Silencing circRNA-ZFAND6 inhibits the proliferation and promotes the apoptosis of HTR8/SVneo cells

In order to explore the biological role of circRNA-ZFAND6, we carried out functional assays. Firstly, we constructed three different siRNAs (si-circ_1, si-circ_2, si-circ_3) targeting circRNA-ZFAND6. Results of RT-qPCR suggested that circRNA-ZFAND6 expression was most significantly decreased in cells transfected with si-circ_1 (Fig. S1), therefore, we chose si-circ_1 (si-circZFAND6) for the following experiments. We constructed circRNA-ZFAND6 over-expression plasmids (circZFAND6) to further determine whether overexpression of circRNA-ZFAND6 has the opposite effects. CCK-8 and EdU assays showed that silencing circRNA-ZFAND6 reduced the proliferation of HTR-8/SVneo cells (Fig. 2A and B). Then, flow cytometry assay prompted that si-circZFAND6 obviously accelerated cells apoptosis (Fig. 2C). Moreover, to assess the migration and invasion abilities of the treated HTR-8/SVneo cells, we conducted scratch wound healing and transwell assays. Results showed no obvious changes (Fig. 2D and E). Overexpression of circRNA-ZFAND6 promoted the proliferation and inhibited the apoptosis of cells, and similarly had no effect on cell migration and invasion (Fig. 2A-E). So as to further explore the potential molecular mechanisms that promote cell apoptosis, we measured the expression levels of proteins related to apoptosis. Results demonstrated that si-circZFAND6 increased the protein expression level of pro-apoptotic genes, such as Bax, caspase9, cleaved-caspase3, compared with si-NC group. Also, Bcl-2, a classic anti-apoptotic protein, significantly decreased after silencing circRNA-ZFAND6 (Fig. 2F). The results revealed that the changes of protein expression after overexpression of circRNA-ZFAND6 were completely opposite to those of silencing circRNA-ZFAND6 (Fig. 2F). Therefore, we concluded that circRNA-ZFAND6, which was lowly expressed in placental villous tissues of URSA patients, was a novel circRNA with the ability to affect the proliferation and apoptosis of HTR8/SVneo cells.

CircRNA-ZFAND6 serves as a molecular sponge for miR-575 in HTR-8/SVneo cells

In general, the different localization of circRNAs in cells affects its function [27]. FISH assay showed that circRNA-ZFAND6 was mainly distributed in the cytoplasm of HTR-8/SVneo cells (Fig. 1G). CircRNAs located in the cytoplasm often work as competing endogenous RNAs (ceRNAs), acting as "sponges" for adsorbed miRNAs. Thus, they can affect the expression of downstream target genes of those miRNAs [28, 29]. Potential miRNAs binding to circRNA-ZFAND6 were predicted by different databases, we focused on miR-575 as potential targets because according to literature review, it may be related to apoptosis [30]. Previous studies demonstrated that the level of miR-575 was significantly up-regulated in the villous tissue of patients with spontaneous abortion and was related to increased apoptosis of trophoblasts [31, 32]. We validated miR-575 expression level in tissues. The results were consistent with previous studies (Fig. 3A). Preliminary evidence suggested that circRNA-ZFAND6 served as a molecular sponge for miR-575.

MiR-575 inhibits the proliferation and promotes the apoptosis of HTR8/SVneo cells

The biological role of miR-575 in the occurrence and progression of URSA largely remained unknown, so we constructed miR-575 mimics, miR-575 inhibitor and their related control (mimics-NC and inhibitor-NC). Their transfection efficiency was also verified (Fig. 3B). Firstly, we performed a dual-luciferase activity assay to confirm that miR-575 can bind to circRNA-ZFAND6. Wild type (WT) circRNA-ZFAND6 which contains the binding sequences of miR-575 and mutant type (Mut) circRNA-ZFAND6 in which the binding sequences were mutated were cloned into the luciferase reporter vector. HEK-293T cells were co-transfected with the circRNA-ZFAND6-WT or circRNA-ZFAND6-Mut luciferase reporter and miR-575 mimics. The results indicated that miR-575 mimics obviously reduced the luciferase activity of the circRNA-ZFAND6-WT, confirming that miR-575

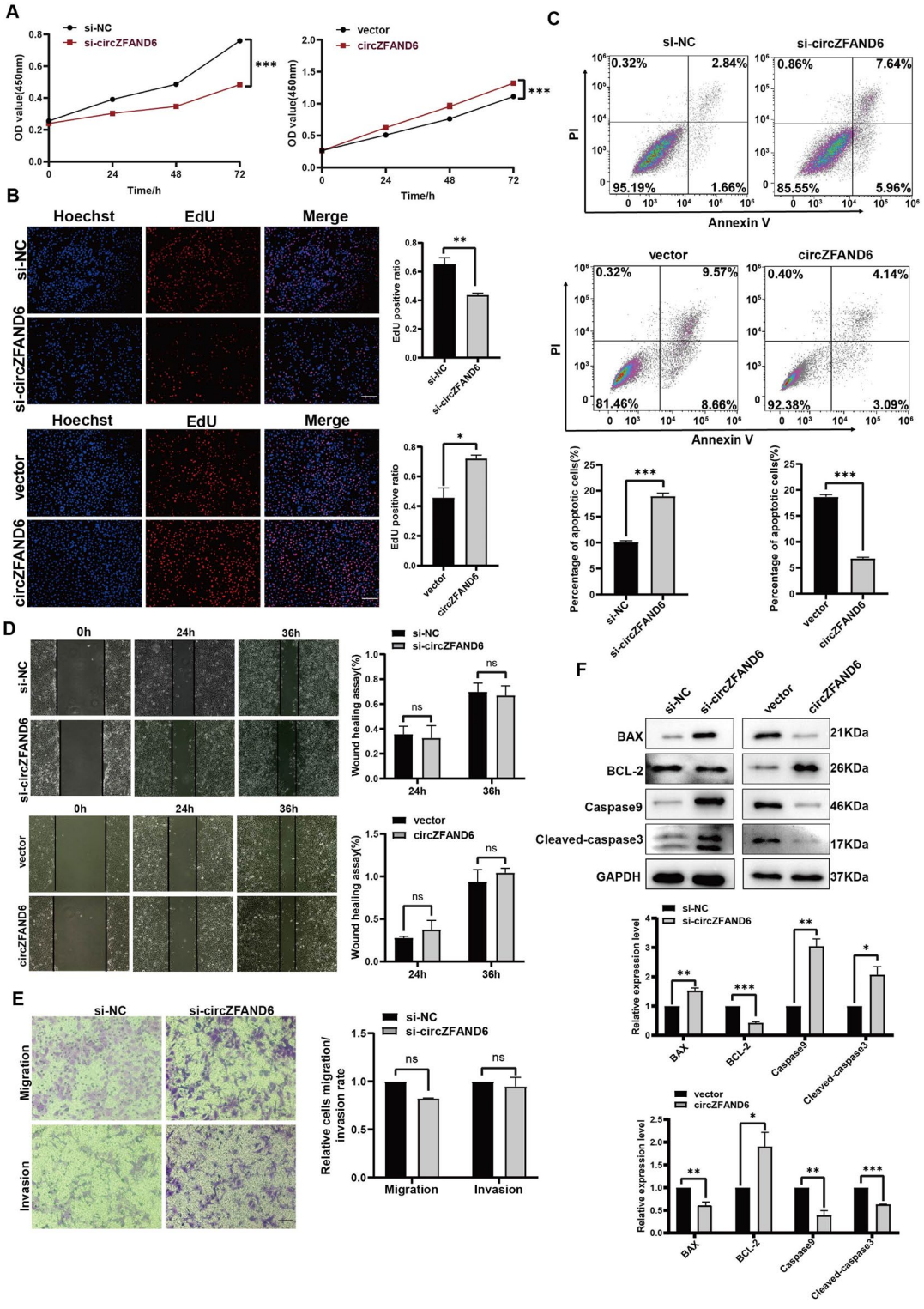

Fig. 2 Silencing circRNA-ZFAND6 inhibits the proliferation and promotes the apoptosis of HTR8/SVneo cells (**A**, **B**) Effects of circRNA-ZFAND6 knockdown or overexpression on cell proliferation were monitored via CCK-8 and EdU assays. Scale bar, 50 μm. (**C**) The apoptotic rate was detected through flow cytometry transfected with si-circZFAND6 or circZFAND6. (**D**) The migration ability was assessed by scratch wound healing assay. Magnification, x40. (**E**) Transwell invasion and migration assay in transfected HTR8/SVneo cells. Scale bar, 100 μm. (**F**) Effects of circRNA-ZFAND6 silencing or overexpression on the levels of apoptosis-related proteinswere measured via western blot assay. GAPDH served as the internal control. Three different independent experiments with three technical repetitions were performed. Data were expressed as the mean ± SEM. * $p<0.05$, ** $p<0.01$, *** $p<0.001$, ns, not significant

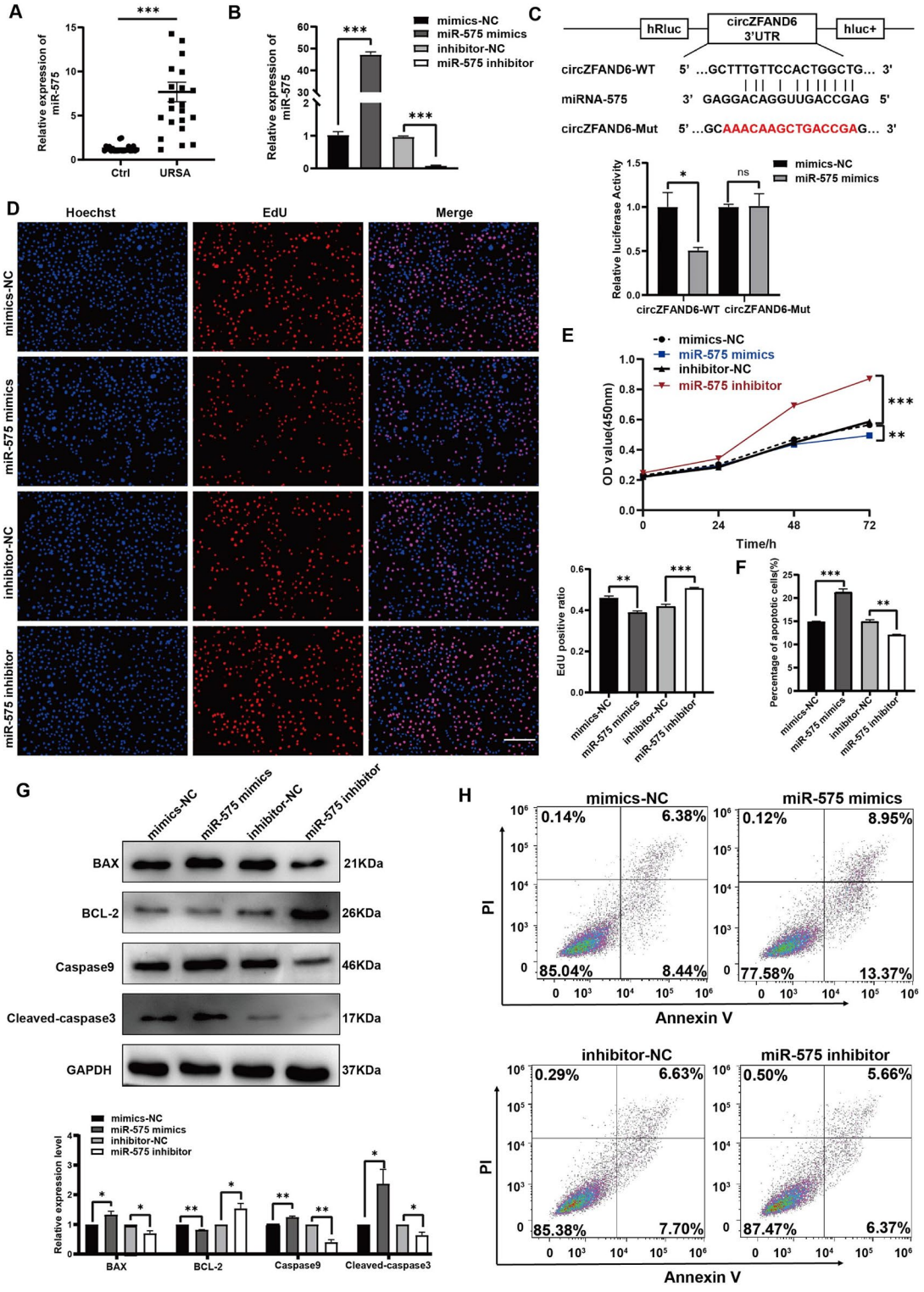

Fig. 3 CircRNA-ZFAND6 serves as a molecular sponge for miR-575and functions of miR-575in HTR8/SVneo cells. (**A**) The level of miR-575 in villus tissues of Ctrl and URSA (n=23) were measured via qRT-PCR. (**B**) RT-qPCR was performed to evaluate the transfection efficiency of miR-575 mimics and miR-575 inhibitor compared with their related control. (**C**) Schematic representation of miR-575 binding sites on circRNA-ZFAND6. The red part was the mutated sequences of circRNA-ZFAND6. Dual-luciferase reporter assay was performed in HEK-293T cells after transfection. (**D**, **E**) EdU and CCK8 analysis of the cell proliferation ability after transfected with miR-575 mimics and miR-575 inhibitor. Scale bar, 50 μm. (**F**, **H**) Flow cytometric analysis of cell apoptosis in treated HTR8/SVneo cells. (**G**) Western blot analysis of the protein expression level of Bax, Bcl-2, caspase9 and cleaved-caspase3 after transfected in HTR8/SVneo cells. GAPDH served as the internal control. Three different independent experiments with three technical repetitions were performed. Data were expressed as the mean ± SEM. * p<0.05, ** p<0.01, *** p<0.001, ns, not significant

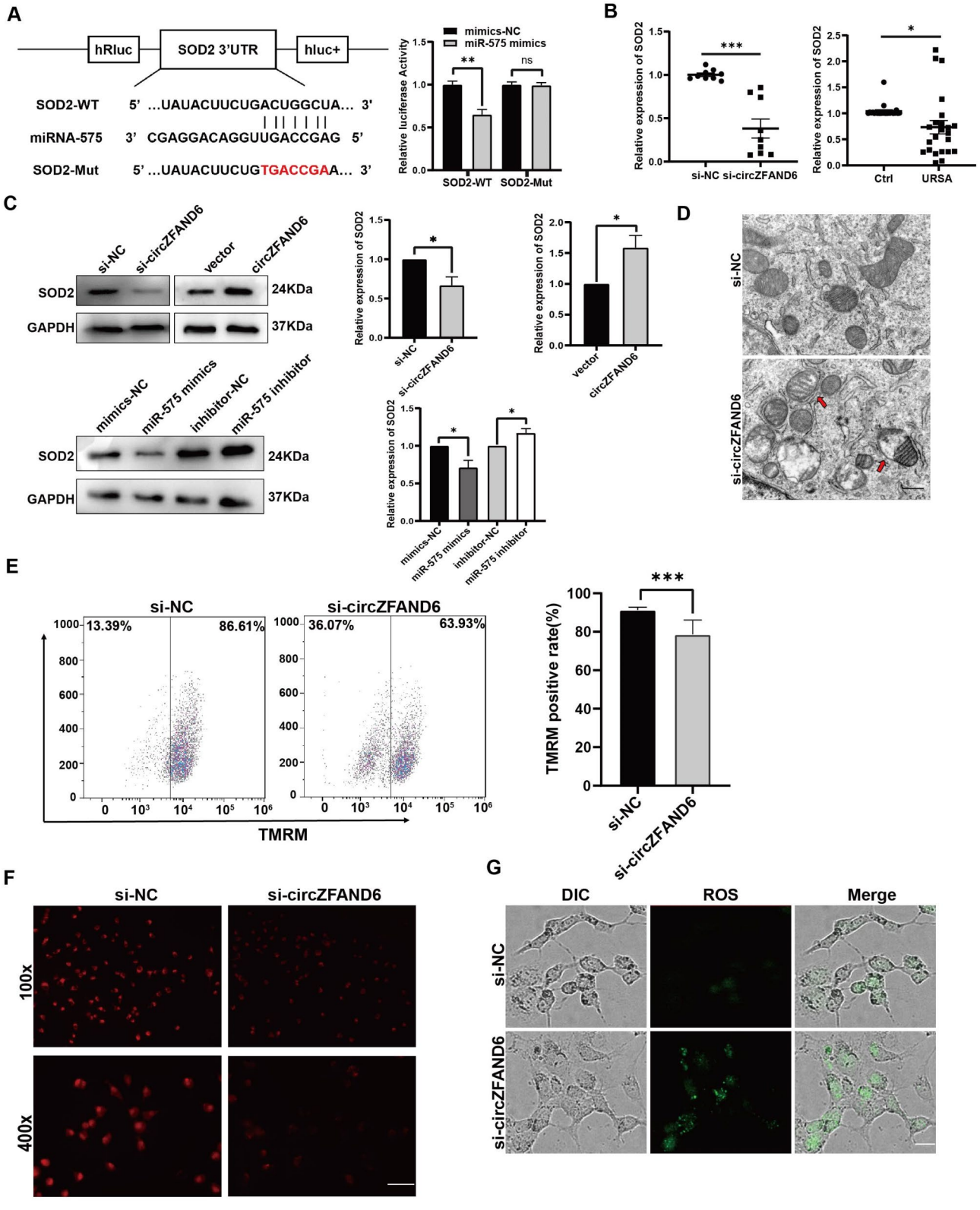

Fig. 4 (See legend on next page.)

(See figure on previous page.)

Fig. 4 SOD2 is a direct target of miR-575. (**A**) Schematic representation of miR-575 binding sites on SOD2. The red part was the mutated sequences of SOD2. Dual-luciferase reporter assay was performed in HEK-293T cells after transfection. (**B**) RT-qPCR analysis of the mRNA expression level of SOD2 in HTR-8/SVneo cells transfected with si-circZFAND6 and in villus tissues of Ctrl and URSA (n=23). (**C**) Western blot analysis of SOD2 protein level in transfected HTR-8/SVneo cells. (**D**) Electron microscope images showed the morphological changes of mitochondriain HTR-8/SVneo cells after silencing circRNA-ZFAND6. Scale bar, 1 μm. (**E**, **F**) Flow cytometry and fluorescence microscopy were used to analyze the changes of mitochondrial membrane potential. (**G**) Fluorescence microscopy was used to analyze the changes of intracellular ROS after transfected with si-circZFAND6. Scale bar, 20 μm. Three different independent experiments with three technical repetitions were performed. Data were expressed as the mean ± SEM. * p<0.05, ** p<0.01, *** p<0.001, ns, not significant

was a direct target of circRNA-ZFAND6 (Fig. 3C). Next, we investigated the function of miR-575. EdU and CCK-8 assays showed that miR-575 mimics curbed and its inhibitor enhanced cell proliferation (Fig. 3D and E). Moreover, flow cytometry assay revealed that miR-575 mimics promoted cell apoptosis whereas its inhibitor suppressed cell apoptosis (Fig. 3F and H). Our western blot studies revealed that pro-apoptotic proteins such as Bax, caspase9 and cleaved-caspase3 increased upon miR-575 mimics treatment. However, their levels were downregulated when treated with miR-575 inhibitors. Furthermore, the level of Bcl-2 in miR-575 mimics group was lower than that in NC group, while the level of Bcl-2 in miR-575 inhibitors group was higher than that in NC group (Fig. 3G).

SOD2 is a direct target of miR-575 and is associated with mitochondrial pathway of apoptosis

The next task was to find the targets of miR-575. According to literature review, miR-575 was mainly focused on the research field of tumor and vascular endothelial cells in the past [33–35], and only one paper reported that miR-575 silencing may affect the apoptosis level of human choriocarcinoma cells, JEG-3, by targeting SOD2 [31]. Thus, we explored whether SOD2 can combine with miR-575. The binding site of miR-575 on SOD2 was shown in Fig. 4A. Dual-luciferase reporter assays suggested that miR-575 can directly bind to SOD2 (Fig. 4A). The expression of SOD2 was significantly reduced after silencing circRNA-ZFAND6. And its expression in villi of URSA group was also significantly reduced (Fig. 4B). SOD2 protein levels were downregulated in cells transfected with si-circZFAND6. Overexpression of circRNA-ZFAND6 showed completely opposite results. Additionally, SOD2 levels were found to be decreased upon miR-575 mimics transfection and increased upon miR-575 inhibitors transfection compared with their corresponding control group (Fig. 4C). To summarize the conclusions above, circRNA-ZFAND6 regulated trophoblast apoptosis by affecting SOD2 expression through adsorbing miR-575. SOD2 is recognized as a mitochondrial antioxidant protein. The abnormal expression of SOD2 may cause oxidative stress injury, mitochondrial apoptosis, and increased apoptosis, which may be involved in miscarriage [36, 37]. Therefore, we further investigated how circRNA-ZFAND6 affected mitochondrial function to induce cell apoptosis. Transmission electron microscopy showed that the mitochondrial spines were significantly reduced, and the mitochondria were swollen cavitation, and irregularly arranged in the trophoblast cells treated with si-circZFAND6 (Fig. 4D). Then, we detect changes in mitochondrial membrane potential by tetramethylrhodamine, methyl ester (TMRM), a cell-permeant dye that accumulates in active mitochondria with intact membrane potentials. TMRM signal was detected with flow cytometry and fluorescence microscopy. The accumulation of TMRM was significantly reduced and the signal was markedly dim or absent after silencing the expression of circRNA-ZFAND6, indicating changes in mitochondrial function and loss of the mitochondrial membrane potential (Fig. 4E and F). Mitochondrial dysfunction can cause excessive production of mitochondrial ROS, which in turn aggravates mitochondrial dysfunction and causes further cell and tissue damage [38]. Here, we use the fluorescent probe DCFH-DA to access the intracellular ROS levels. It was obvious that ROS was found to be increased in circRNA-ZFAND6 silenced cells (Fig. 4G). The above western blot detection of protein involved in mitochondrial apoptosis also suggested that the level of caspase9 and cleaved-caspase3 were significantly increased, while the level of SOD2 and Bcl-2 were decreased in cells treated with si-circZFAND6 (Figs. 2F and 4C). These results suggested that circRNA-ZFAND6 may affect the expression of SOD2 and thus affect mitochondrial apoptosis by regulating miR-575.

We preliminarily verified that circRNA-ZFAND6 sponged miR-575, and the next step we performed several functional rescue experiments to reinforce our conclusions. As depicted by EdU and CCK-8 assay, cell proliferation ability was weakened in si-circZFAND6-transfected cells, while this effect was attenuated by miR-575 inhibitor (Fig. 5A and B). Our flow cytometry data revealed that si-circZFAND6 + inhibitor-NC group showed a higher proportion of early apoptotic cells than the si-circZFAND6 + miR-575 inhibitor group (Fig. 5C). According to the results of western blot, Bax and caspase9 levels were decreased in the si-circZFAND6 + miR-575 inhibitor group compared to that in the si-circZFAND6 + inhibitor-NC group. In contrast, SOD2 and Bcl2 levels were found to be higher in the si-circZFAND6 + miR-575 inhibitor group than in the si-circZFAND6 + inhibitor-NC group. In the same way,

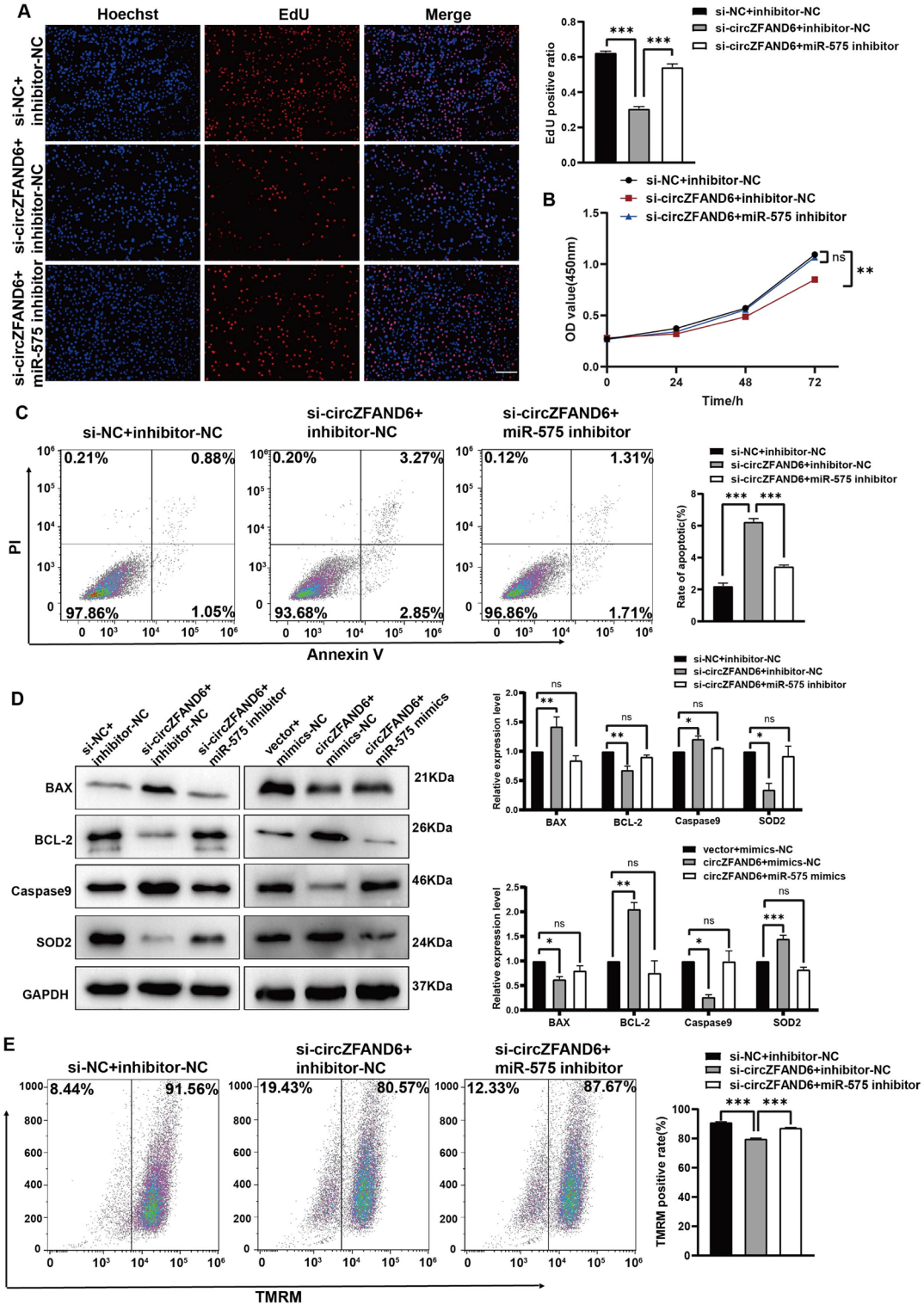

Fig. 5 MiR-575 rescues the effect of circRNA-ZFAND6 in HTR8/SVneo cells. (**A**-**C**) Effects of circRNA-ZFAND6 knockdown on cell proliferation and apoptosis were abrogated by miR-575 inhibitor. Scale bar, 50 μm. (**D**) Western blotting demonstrated the rescue ability of miR-575 inhibitor on circRNA-ZFAND6 knockdown and the rescue abilityof miR-575 mimics on circRNA-ZFAND6 overexpression in HTR8/SVneo cells. Protein levels of Bax, Bcl-2, caspase9, cleaved-caspase3 were determined. GAPDH served as the internal control. (**E**) Flow cytometry analysis showed that miR-575 inhibitor rescued the change of mitochondrial membrane potential caused by si-circZFAND6. Three different independent experiments with three technical repetitions were performed. Data were expressed as the mean ± SEM. * $p<0.05$, ** $p<0.01$, *** $p<0.001$, ns, not significant. MiR-575 inhibitor rescues the effect of circRNA-ZFAND6 silencing in HTR8/SVneo cells

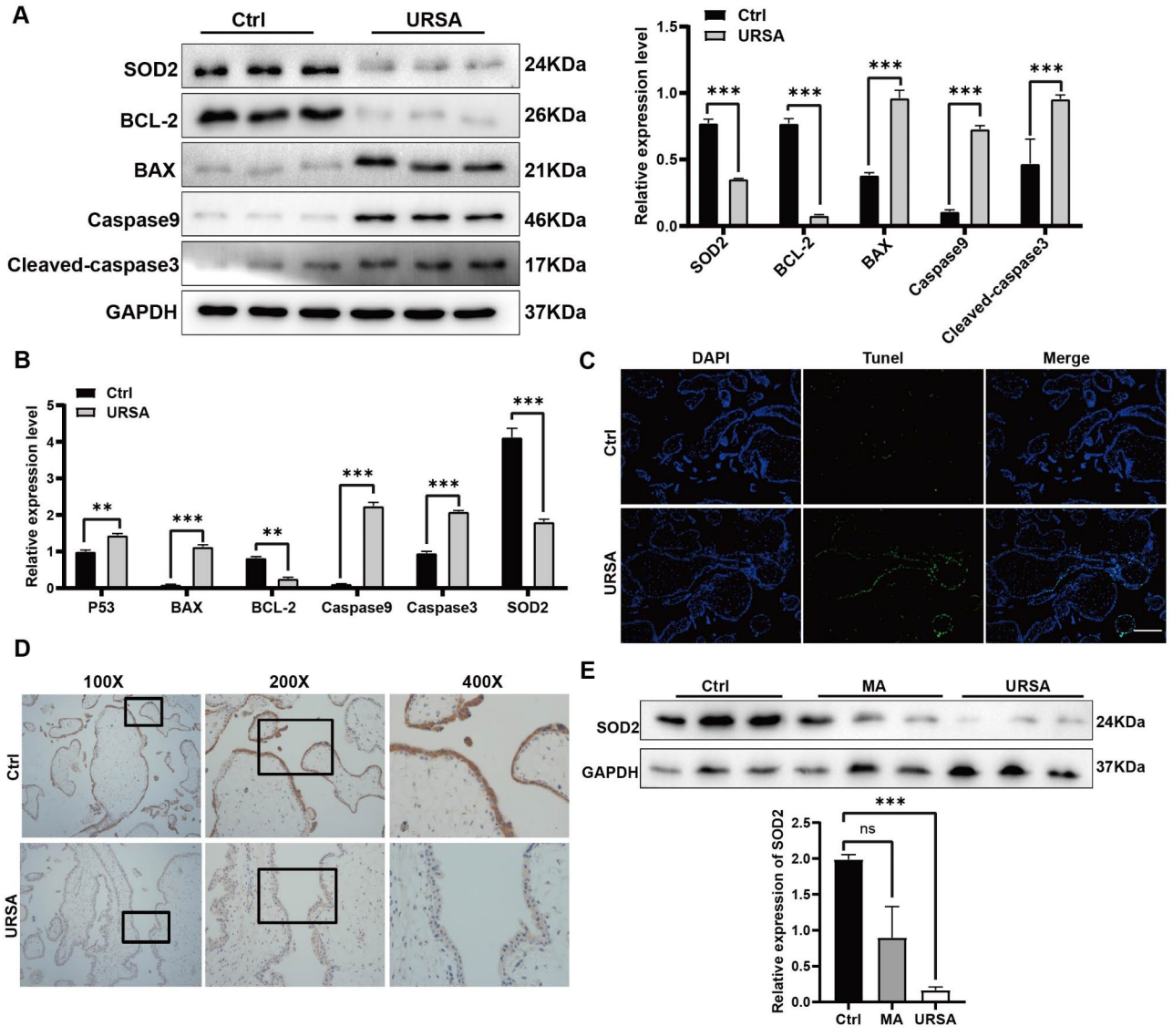

Fig. 6 The placental trophoblast apoptosis of URSA increased significantly. (**A**) Western blot analysis of the expression level of apoptosis-related proteins in villus tissues of Ctrl and URSA group (n=3). GAPDH served as the internal control. (**B**) RT-qPCR assay was performed to evaluate the mRNA expression of apoptosis-related genesin villus tissues of Ctrl and URSA group (n=3). (**C**) Tunel staining of villus tissues from Ctrl and URSA group (n=3). (**D**) SOD2 protein expression was detected by immunohistochemistry (IHC) in Ctrl and URSA villus tissues (n=3). Representative images of SOD2 expression detected by IHC assays were shown. (**E**) Western blot analysis of the protein expression level of SOD2 in 3 groups of villus tissues of Ctrl, MA and URSA group. Three different independent experiments with three technical repetitions were performed. Data were expressed as the mean ± SEM. * p<0.05, ** p<0.01, *** p<0.001, ns, not significant

miR-575 mimics could partially abolish circZFAND6 mediated increase of SOD2 and Bcl2 and restored circZFAND6 mediated suppression of Bax and caspase9 at protein levels (Fig. 5D). Flow cytometry was also shown that miR-575 inhibitor reduced the change of cell membrane potential caused by si-circZFAND6 (Fig. 5E). Taken together, the rescue experiments showed that miR-575 could partially reverse the effects of circRNA-ZFAND6 alterations on trophoblast proliferation and apoptosis. CircRNA-ZFAND6 can play a role of ceRNA and affect the expression of SOD2 by binding to miR-575.

CircRNA-ZFAND6 is involved in the occurrence of URSA by regulating mitochondrial apoptosis in trophoblast cells

Next, we analyzed the change of mitochondrial apoptosis related gene and protein levels in the placental villi tissue of URSA and Ctrl group. We found that the apoptosis of trophoblast cells in the placental villi of URSA group was higher than that of Ctrl group and may be related to mitochondrial dysfunction (Fig. 6A and B). Results of Tunel staining displayed that the number of Tunel-positive cells in URSA group markedly increased (Fig. 6C), suggesting an increase in cell apoptosis. SOD2 protein

expression was measured by immunohistochemistry (IHC) and western blot in URSA and Ctrl placental villus. Results revealed that SOD2 expression was lower in URSA samples (Fig. 6D and E). In addition, the reduction of SOD2 protein level in placental villus tissues of URSA group was more significant than that of the group experiencing missed abortion for the first time (Fig. 6E). These evidences indicated that excessive trophoblast apoptosis can lead to trophoblast dysfunction and promote the development of URSA. Further, we need to attach importance to the recurrence risk of miscarriage.

Discussion

CircRNAs have been reported to regulate cellular functions and participate in the progression of many diseases [39, 40]. Several circRNAs have been proved to be connected to the pathophysiological processes of URSA [41]. For example, downregulation of circHIPK3 (hsa_circ_0000284) expression in URSA weakened proliferation and migration of trophoblasts through regulating miR-30a-3p/Wnt2 axis [42]. CircRNA-0050703, known as circRNA-DURSA, was an obvious downregulated circRNA in URSA placental villus. It can act as a sponge for miR-760, alleviating its inhibition of HIST1H2BE expression and protecting trophoblast cells from apoptosis [25]. In this study, we put our attention on hsa_circ_0000643 whose function remained largely unknow. It originated from the back-splice of ZFAND6 exons 2, 3 and 4. It was a completely novel circRNA and we renamed it circRNA-ZFAND6 to carry out further exploration. Consistent with the results shown by the microarray results, circRNA-ZFAND6 expression was obviously reduced in placental villus tissues of URSA group compared with that of normal pregnancy group. We confirmed that circRNA-ZFAND6 was a circular RNA with high stability and was mainly distributed in the cytoplasm. Various biological function assays showed that circRNA-ZFAND6 promoted the proliferation and inhibited the apoptosis of HTR-8/SVneo cells. The above evidence suggested that circRNA-ZFAND6 had the ability to regulate trophoblast proliferation and apoptosis.

The biological functions of circRNAs have been studied widely. CircRNAs, which are known to localize in the cytoplasm, usually play the role of competing endogenous RNAs (ceRNAs). They contain various binding sites of miRNAs. It allows them to function as miRNA sponges, thereby affecting the expression of downstream target genes [43, 44]. Bioinformatics tools along with results from dual-luciferase reporter assays both revealed that miR-575 was able to bind to circRNA-ZFAND6. MiR-575 was significantly upregulated in URSA. Previous studies have identified miR-575 as an oncogene in various cancers, such as Gallbladder Cancer [30], Gastric cancer [33], thyroid cancer [45] and Glioma [46], etc. The above numerous articles showed that miR-575 regulated the proliferation, migration, invasion, apoptosis, inflammatory response and angiogenesis of different cells. We concluded that miR-575 mimics suppressed HTR-8/SVneo cells growth and promoted its apoptosis. On the contrary, miR-575 inhibitor enhanced the proliferation and refrained the apoptosis of the cells. A series of rescue experiments were carried out to further confirm whether the biological function of circRNA-ZFAND6 was associated with miR-575, results revealed that circRNA-ZFAND6 could affect the apoptosis of trophoblast cells by adsorbing miR-575. At present, only one paper reported that miR-575 silencing may reduce the level of apoptosis in a human trophoblastic tumor cell line (JEG-3) by targeting SOD2 [31]. The level of SOD2 protein were detected by circRNA-ZFAND6 silencing and miR-575 overexpressing experiment, and the results both showed that SOD2 protein were significantly downregulated. Moreover, dual-luciferase reporter assays verified that miR-575 can interact with SOD2 directly. To conclude, circRNA-ZFAND6 may regulate the expression of SOD2 by competitive binding to miR-575. SOD2 is recognized as a mitochondrial antioxidant protein and is of vital importance in normal embryonic development. Animal experiments have found that SOD2 homozygous knockout mice can cause fetal death, while SOD2 heterozygous mice have significantly increased oxidative stress and apoptosis levels in various tissues [36, 47]. The abnormal expression of SOD2 is bound up with oxidative stress injury, mitochondrial apoptosis, and increased apoptosis, which may be involved in URSA [48, 49].

Placental trophoblast cells are the main executor of embryo implantation in the establishment and maintenance of normal pregnancy [50]. The normal function of trophoblast is needed for a successful pregnancy. Reduced trophoblast proliferation and excessive trophoblast cell apoptosis have been tightly linked to URSA development [51]. Mitochondria are involved in and play key roles in many cellular processes, including intracellular calcium homeostasis, energy metabolism and apoptosis [52]. As a classical form of programmed cell death, the intrinsic apoptotic pathway of cells plays a universal role in the occurrence of apoptosis [53]. Bcl-2 protein family functions in the process of apoptosis and activates caspase family proteins. The change in expression of Bax (pro-apoptotic protein) and Bcl-2 (anti-apoptotic protein) are causes of apoptosis [54]. The imbalance between pro-apoptotic and anti-apoptotic proteins of the Bcl-2 family increases mitochondrial permeability, activating the caspase family and inducing apoptosis. Caspases are the central components in the execution of apoptosis [38]. Caspase9 is the initiator caspase in the mitochondrial pathway. Caspase3, the downstream caspase of caspase9, is the most critical executing protein of apoptosis

and upon activation, cleaved-caspase3 is formed. Our western blot studies revealed that pro-apoptotic proteins such as Bax, caspase9 and cleaved-caspase3 increased upon silencing circRNA-ZFAND6 or overexpressing miR-575. Furthermore, the level of Bcl-2 was reduced upon overexpressing circRNA-ZFAND6 or silencing miR-575 compared to the control group. Meanwhile, mitochondrial apoptosis related gene and protein levels was significantly increased in the placental villi tissue of URSA group compared with the Ctrl group.

Mitochondrial dysfunction in trophoblast cells was considered to responsible for the apoptosis occurrence. After silencing the expression of circRNA-ZFAND6, the morphology of mitochondria was significantly changed, the membrane potential was decreased, and the intracellular ROS was accumulated. Furthermore, the decrease of Bcl-2 protein level and the increase of Bax, caspase9, cleaved-caspase3 protein levels in si-circZFAND6-treated cells further hinted the activation of mitochondria-mediated apoptosis pathway was involved in the occurrence of apoptosis. We found that the decrease in the level of SOD2 protein in the URSA group was accompanied by impaired mitochondria. Activation of the mitochondria-mediated apoptotic cascade in trophoblast cells may be responsible for the occurrence of apoptosis [52]. SOD2 may be involved in URSA by inducing trophoblast apoptosis through a mitochondria-dependent pathway. In addition, we collected placental villus tissue from patients who experienced missed abortion for the first time, and the reduction of circRNA-ZFAND6 was more pronounced in URSA patients and subsequently had a greater impact on SOD2, which also provided a basis for the greater possibility of RSA with the increase in the number of miscarriages. Therefore, we emphasize the exploration of the etiology of URSA in order to reduce the risk of RSA and protect female fertility. Although our study finally confirmed that the effects of circRNA-ZFAND6 on apoptosis of trophoblast cells, there were certain limitations. Firstly, the function of circRNA-ZFAND6 in HTR-8/SVneo cells does not conclusively prove the pathogenesis of circRNA-ZFAND6 regulating URSA. In future experiments, animal models should be constructed to investigate the role of circRNA-ZFAND6 in vivo. Secondly, circRNA-ZFAND6 may function by mechanisms that are not limited to ceRNA or by binding to other miRNAs. Nonetheless, SOD2 is involved in the mechanism of trophoblast apoptosis and the occurrence of RSA, further identification is still needed. However, the mitochondria-mediated apoptotic pathway undoubtedly opens new ideas for understanding URSA.

Conclusion

CircRNA-ZFAND6 is a lowly expressed circRNA in URSA tissues. It regulates the expression of SOD2 protein by adsorptive miR-575 and participates in the development of URSA through mitochondrial mediated apoptosis. It provides a theoretical basis for understanding the molecular mechanism of circRNA-ZFAND6 and elucidating potential therapeutic targets in URSA. This regulatory mechanism also provides a new theoretical basis for understanding the occurrence and development mechanism of URSA.

Abbreviations

URSA	Unexplained recurrent spontaneous abortion
circRNAs	Circular RNAs
miRNA	MicroRNA
mRNA	Messenger ribonucleic acid
ceRNA	Competing endogenous RNA
si-RNA	Small interfering RNA
RT-qPCR	Reverse transcription-quantitative polymerase chain reaction
CCK-8	Cell counting kit- 8
EdU	5-Ethynyl-2′- deoxyuridine
BMI	Body mass index
FISH	Fluorescent in situ hybridization
DAPI	4′, 6-diamidino-2-phenylindole
GAPDH	Glyceraldehyde-3-phosphate dehydrogenase
HRP	Horseradish peroxidase
UTR	Untranslated region

Supplementary Information

The online version contains supplementary material available at https://doi.org/10.1186/s12905-025-03682-7.

Supplementary Material 1

Supplementary Material 2

Acknowledgements

Not applicable.

Author contributions

WW, ZM and QC conceived of the study and carried out its design. WW wrote the first version of the manuscript. WW, LH and SL performed the experiments. WW, JL and SL conducted the statistical analysis and constructed the figures. SJ collected clinical samples and were involved in the clinical data analysis. QC and SL revised the paper. All authors contributed to revising the manuscript, and approved the final manuscript.

Funding

This work was supported by the Nanjing Medical Science and Technique Development Foundation (ZKX21049).

Data availability

No datasets were generated or analysed during the current study.

Declarations

Ethics approval and consent to participate

The research protocol was approved by the Ethical Committee of Nanjing Maternity and Child Health Care Hospital (No. [2021] NFKSL-076). Written informed consent was collected from all participants before the procedure.

Consent for publication

Not applicable.

Competing interests
The authors declare no competing interests.

Author details
[1]Nanjing Maternity and Child Health Care Hospital, Women's Hospital of Nanjing Medical University, Nanjing, Jiangsu 210004, China

Received: 24 November 2023 / Accepted: 20 March 2025
Published online: 08 April 2025

References

1. Bender AR, Christiansen OB, Elson J, Kolte AM, Lewis S, Middeldorp S, et al. Eshre guideline: recurrent pregnancy loss: an update in 2022. Hum Reprod Open 2023. 2023;2023(1):d2. https://doi.org/10.1093/hropen/hoad002.
2. Evaluation. and treatment of recurrent pregnancy loss: a committee opinion. Fertil Steril. 2012 2012;98(5):1103-11. https://doi.org/10.1016/j.fertnstert.2012.06.048
3. Dimitriadis E, Menkhorst E, Saito S, Kutteh WH, Brosens JJ. Recurrent pregnancy loss. Nat Rev Dis Primers. 2020 2020;6(1):98. https://doi.org/10.1038/s41572-020-00228-z
4. Chen P, Zhou L, Chen J, Lu Y, Cao C, Lv S, et al. The immune atlas of human deciduas with unexplained recurrent pregnancy loss. Front Immunol. 2021;2021(12):689019. https://doi.org/10.3389/fimmu.2021.689019.
5. El HH, Crepaux V, May-Panloup P, Descamps P, Legendre G, Bouet PE. Recurrent pregnancy loss: current perspectives. Int J Womens Health 2017. 2017;9:331–45. https://doi.org/10.2147/IJWH.S100817.
6. Gu H, Li L, Du M, Xu H, Gao M, Liu X et al. Key gene and functional pathways identified in unexplained recurrent spontaneous abortion using targeted rna sequencing and clinical analysis. Front Immunol. 2021 2021;12:717832. https://doi.org/10.3389/fimmu.2021.717832
7. Jaslow CR, Carney JL, Kutteh WH. Diagnostic factors identified in 1020 women with two versus three or more recurrent pregnancy losses. Fertil Steril. 2010 2010;93(4):1234-43. https://doi.org/10.1016/j.fertnstert.2009.01.166
8. van Dijk MM, Kolte AM, Limpens J, Kirk E, Quenby S, van Wely M et al. Recurrent pregnancy loss: diagnostic workup after two or three pregnancy losses? A systematic review of the literature and meta-analysis. Hum Reprod Update. 2020 2020;26(3):356– 67. https://doi.org/10.1093/humupd/dmz048
9. Youssef A, Lashley L, Dieben S, van der Verburg H. Defining recurrent pregnancy loss: associated factors and prognosis in couples with two versus three or more pregnancy losses. Reprod Biomed Online 2020. 2020;41(4):679–85. https://doi.org/10.1016/j.rbmo.2020.05.016.
10. Egerup P, Kolte AM, Larsen EC, Krog M, Nielsen HS, Christiansen OB. Recurrent pregnancy loss: what is the impact of consecutive versus non-consecutive losses? Hum Reprod 2016. 2016;31(11):2428–34. https://doi.org/10.1093/humrep/dew169.
11. Zhu D, Zou H, Liu J, Wang J, Ma C, Yin J et al. Inhibition of hmgb1 ameliorates the maternal-fetal interface destruction in unexplained recurrent spontaneous abortion by suppressing pyroptosis activation. Front Immunol. 2021 2021;12:782792. https://doi.org/10.3389/fimmu.2021.782792
12. Shi Y, Wang Q, Song R, Kong Y, Zhang Z. Non-coding Rnas in depression: promising diagnostic and therapeutic biomarkers. Ebiomedicine 2021. 2021;71:103569. https://doi.org/10.1016/j.ebiom.2021.103569.
13. Liu X, Wu J, Nie H, Zhu X, Song G, Han L et al. Comprehensive analysis of circrnas, mirnas, and mrnas expression profiles and cerna networks in decidua of unexplained recurrent spontaneous abortion. Front Genet. 2022 2022;13:858641. https://doi.org/10.3389/fgene.2022.858641
14. Qin W, Tang Y, Yang N, Wei X, Wu J. Potential role of Circulating Micrornas as a biomarker for unexplained recurrent spontaneous abortion. Fertil Steril 2016. 2016;105(5):1247–54. https://doi.org/10.1016/j.fertnstert.2016.01.028.
15. Patop IL, Wüst S, Kadener S. Past, present, and future of circrnas. Embo J 2019. 2019;38(16):e100836. https://doi.org/10.15252/embj.2018100836.
16. Hansen TB, Jensen TI, Clausen BH, Bramsen JB, Finsen B, Damgaard CK, et al. Natural Rna circles function as efficient Microrna sponges. Nat 2013. 2013;495(7441):384–88. https://doi.org/10.1038/nature11993.
17. Meng S, Zhou H, Feng Z, Xu Z, Tang Y, Li P, et al. Circrna: functions and properties of a novel potential biomarker for cancer. Mol Cancer 2017. 2017;16(1):94. https://doi.org/10.1186/s12943-017-0663-2.
18. Chen X, Guo DY, Yin TL, Yang J. Non-coding Rnas regulate placental trophoblast function and participate in recurrent abortion. Front Pharmacol 2021. 2021;12:646521. https://doi.org/10.3389/fphar.2021.646521.
19. Zhu L, Shi L, Ye W, Li S, Liu X, Zhu Z. Circular Rna pum1 (circpum1) attenuates trophoblast cell dysfunction and inflammation in recurrent spontaneous abortion via the microrna-30a-5p (mir-30a-5p)/junb axis. Bioengineered 2021. 2021;12(1):6878–90. https://doi.org/10.1080/21655979.2021.1973207.
20. Gao Y, Tang Y, Sun Q, Guan G, Wu X, Shi F, et al. Circular Rna foxp1 relieves trophoblastic cell dysfunction in recurrent pregnancy loss via the mir-143-3p/s100a11 cascade. Bioengineered 2021. 2021;12(1):9081–93. https://doi.org/10.1080/21655979.2021.1988374.
21. Liu J, Zhang Z, Zhu W, Shen Y, Gu Y, Zhang X, et al. Circfbxw4 regulates human trophoblast cell proliferation and invasion via targeting mir-324-3p/tjp1 axis in recurrent spontaneous abortion. Placenta 2022. 2022;126:1–11. https://doi.org/10.1016/j.placenta.2022.05.016.
22. Ticconi C, Pietropolli A, Di Simone N, Piccione E, Fazleabas A. Endometrial immune dysfunction in recurrent pregnancy loss. Int J Mol Sci 2019. 2019;20(21). https://doi.org/10.3390/ijms20215332.
23. Abbas Y, Turco MY, Burton GJ, Moffett A. Investigation of human trophoblast invasion in vitro. Hum Reprod Update 2020. 2020;26(4):501–13. https://doi.org/10.1093/humupd/dmaa017.
24. Zhang Y, Zhou J, Li MQ, Xu J, Zhang JP, Jin LP. Microrna-184 promotes apoptosis of trophoblast cells via targeting wig1 and induces early spontaneous abortion. Cell Death Dis 2019. 2019;10(3):223. https://doi.org/10.1038/s41419-019-1443-2.
25. Tang M, Bai L, Wan Z, Wan S, Xiang Y, Qian Y et al. Circrna-dursa regulates trophoblast apoptosis via mir-760-hist1h2be axis in unexplained recurrent spontaneous abortion. Mol Ther Nucleic Acids. 2021 2021;26:1433-45. https://doi.org/10.1016/j.omtn.2021.06.012
26. Qian Y, Wang X, Ruan H, Rui C, Mao P, Cheng Q, et al. Circular Rnas expressed in chorionic villi are probably involved in the occurrence of recurrent spontaneous abortion. Biomed Pharmacother. 2017;88(Complete):1154–62.
27. Ma C, Wang X, Yang F, Zang Y, Liu J, Wang X, et al. Circular Rna Hsa_circ_0004872 inhibits gastric cancer progression via the mir-224/smad4/adar1 successive regulatory circuit. Mol Cancer 2020. 2020;19(1):157. https://doi.org/10.1186/s12943-020-01268-5.
28. Jing MY, Xie LD, Chen X, Zhou Y, Jin MM, He WH et al. Circ-ccnb1 modulates trophoblast proliferation and invasion in spontaneous abortion by regulating mir-223/siah1 axis. Endocrinology. 2022 2022;163(8). https://doi.org/10.1210/endocr/bqac093
29. Luo Z, Rong Z, Zhang J, Zhu Z, Yu Z, Li T, et al. Circular Rna circccdc9 acts as a mir-6792-3p sponge to suppress the progression of gastric cancer through regulating cav1 expression. Mol Cancer 2020. 2020;19(1):86. https://doi.org/10.1186/s12943-020-01203-8.
30. Qin Y, Mi W, Huang C, Li J, Zhang Y, Fu Y. Downregulation of mir-575 inhibits the tumorigenesis of gallbladder cancer via targeting p27 kip1. Onco Targets Ther. 2020 2020;13:3667-76. https://doi.org/10.2147/OTT.S229614
31. Xia S, Zhen Y, Ma H, Wang A. Abnormal expression of microrna-575 leads to missed abortion through regulating apoptosis and angiogenesis. Exp Ther Med. 2017 2017;14(5):3993–4000. https://doi.org/10.3892/etm.2017.5086
32. Hosseini MK, Gunel T, Gumusoglu E, Benian A, Aydinli K. Microrna expression profiling in placenta and maternal plasma in early pregnancy loss. Mol Med Rep 2018. 2018;17(4):4941–52. https://doi.org/10.3892/mmr.2018.8530.
33. Wang YN, Xu F, Zhang P, Wang P, Wei YN, Wu C, et al. Microrna-575 regulates development of gastric cancer by targeting Pten. Biomed Pharmacother 2019. 2019;113:108716. https://doi.org/10.1016/j.biopha.2019.108716.
34. Zhao X, Yi Y, Meng C, Fang N. Mirna-575 suppresses angiogenesis by targeting rab5-mek-erk pathway in endothelial cells. Biosci Rep 2019. 2019;39(1). https://doi.org/10.1042/BSR20181218.
35. Luan X, Yan Y, Zheng Q, Wang M, Chen W, Yu J, et al. Excessive reactive oxygen species induce apoptosis via the appl1-nrf2/ho-1 antioxidant signalling pathway in trophoblasts with missed abortion. Life Sci 2020. 2020;254:117781. https://doi.org/10.1016/j.lfs.2020.117781.
36. Zhang Y, Zhang HM, Shi Y, Lustgarten M, Li Y, Qi W et al. Loss of manganese superoxide dismutase leads to abnormal growth and signal transduction in mouse embryonic fibroblasts. Free Radic Biol Med. 2010 2010;49(8):1255-62. https://doi.org/10.1016/j.freeradbiomed.2010.07.006
37. Zejnullahu VA, Zejnullahu VA, Kosumi E. The role of oxidative stress in patients with recurrent pregnancy loss: a review. Reprod Health 2021. 2021;18(1):207. https://doi.org/10.1186/s12978-021-01257-x.
38. Yang X, Xue P, Chen H, Yuan M, Kang Y, Duscher D et al. Denervation drives skeletal muscle atrophy and induces mitochondrial dysfunction, mitophagy

and apoptosis via mir-142a-5p/mfn1 axis. Theranostics. 2020 2020;10(3):1415-32. https://doi.org/10.7150/thno.40857
39. Dong Y, He D, Peng Z, Peng W, Shi W, Wang J, et al. Circular Rnas in cancer: an emerging key player. J Hematol Oncol 2017. 2017;10(1):2. https://doi.org/10.1186/s13045-016-0370-2.
40. Han B, Chao J, Yao H. Circular Rna and its mechanisms in disease: from the bench to the clinic. Pharmacol Ther 2018. 2018;187:31–44. https://doi.org/10.1016/j.pharmthera.2018.01.010.
41. Wang Y, Cheng Q, Xia Z, Zhou R, Li Y, Meng L, et al. Whole-transcriptome sequencing identifies key Mrnas, Mirnas, Lncrnas, and circrnas associated with unexplained recurrent pregnancy loss. Cell Tissue Res 2022. 2022;389(1):129–43. https://doi.org/10.1007/s00441-022-03632-x.
42. Li S, Li N, Li B, Zhu L, Xu T, Wang L et al. Circhipk3 promotes proliferation and metastasis of villous trophoblasts through mir-30a-3p/wnt2 axis. J Genet. 2022 2022;101.
43. Yang S, Wang X, Zhou X, Hou L, Wu J, Zhang W et al. Ncrna-mediated cerna regulatory network: transcriptomic insights into breast cancer progression and treatment strategies. Biomed Pharmacother. 2023 2023;162:114698. https://doi.org/10.1016/j.biopha.2023.114698
44. Chen L, Wang C, Sun H, Wang J, Liang Y, Wang Y, et al. The bioinformatics toolbox for circrna discovery and analysis. Brief Bioinform 2021. 2021;22(2):1706–28. https://doi.org/10.1093/bib/bbaa001.
45. Dong H, Wu YL, Zhang X, Li HL, Zheng WH. Microrna-575 targets Derlin 1 to regulate proliferation, migration and invasion of human thyroid cancer cells. Arch Med Sci 2023. 2023;19(4):1108–15. https://doi.org/10.5114/aoms.2020.92867.
46. Wei G, Li S, Wang P, Wang S, Zhao Y. Altered expression of mir-575 in glioma is related to tumor cell proliferation, migration, and invasion. Neuromolecular Med. 2022 2022;24(2):224– 31. https://doi.org/10.1007/s12017-021-08679-7
47. Zaidi SK, Shen WJ, Cortez Y, Bittner S, Bittner A, Arshad S, et al. Sod2 deficiency-induced oxidative stress attenuates steroidogenesis in mouse ovarian granulosa cells. Mol Cell Endocrinol 2021. 2021;519:110888. https://doi.org/10.1016/j.mce.2020.110888.
48. Ghneim HK, Al-Sheikh YA, Alshebly MM, Aboul-Soud MA. Superoxide dismutase activity and gene expression levels in Saudi women with recurrent miscarriage. Mol Med Rep 2016. 2016;13(3):2606–12. https://doi.org/10.3892/mmr.2016.4807.
49. Al-Sheikh YA, Ghneim HK, Alharbi AF, Alshebly MM, Aljaser FS, Aboul-Soud M. Molecular and biochemical investigations of key antioxidant/oxidant molecules in saudi patients with recurrent miscarriage. Exp Ther Med. 2019 2019;18(6):4450-60. https://doi.org/10.3892/etm.2019.8082
50. Liang L, Chen Y, Wu C, Cao Z, Xia L, Meng J, et al. Microrna: key regulators of the trophoblast function in pregnancy disorders. J Assist Reprod Genet 2023. 2023;40(1):3–17. https://doi.org/10.1007/s10815-022-02677-9.
51. Liu Z, Tang Y, Zhang X, Pei J, Wang C, Liu H, et al. Crosstalk between placental trophoblast and decidual immune cells in recurrent miscarriage. Int J Med Sci 2023. 2023;20(9):1174–88. https://doi.org/10.7150/ijms.86533.
52. Pang W, Zhang Y, Zhao N, Darwiche SS, Fu X, Xiang W. Low expression of mfn2 is associated with mitochondrial damage and apoptosis in the placental villi of early unexplained miscarriage. Placenta 2013. 2013;34(7):613–18. https://doi.org/10.1016/j.placenta.2013.03.013.
53. Huang Y, Dong F, Du Q, Zhang H, Luo X, Song X, et al. Swainsonine induces apoptosis through mitochondrial pathway and caspase activation in goat trophoblasts. Int J Biol Sci 2014. 2014;10(7):789–97. https://doi.org/10.7150/ijbs.9168.
54. Aamazadeh F, Ostadrahimi A, Rahbar SY, Barar J. Bitter apricot ethanolic extract induces apoptosis through increasing expression of bax/bcl-2 ratio and caspase-3 in panc-1 pancreatic cancer cells. Mol Biol Rep 2020. 2020;47(3):1895–904. https://doi.org/10.1007/s11033-020-05286-w.

Publisher's note